의학박사 학위논문

Evaluation of cerebral blood flow changes associated with cerebral hypoxia-ischemia in neonatal rats using arterial spin labeling perfusion MRI

신생 백서를 이용한 저산소성 허혈성 뇌손상 모델에서 동맥스핀표지 관류 자기공명영상법을 통한 뇌혈류 변화 평가

2020 년 2 월

서울대학교 대학원

의학과 영상의학전공

최 영 훈

Evaluation of cerebral blood flow changes associated with cerebral hypoxia-ischemia in neonatal rats using arterial spin labeling perfusion MRI

신생 백서를 이용한 저산소성 허혈성 뇌손상 모델에서 동맥스핀표지 관류 자기공명영상법을 통한 뇌혈류 변화 평가

지도교수 천 정 은

이 논문을 의학박사 학위논문으로 제출함

2019 년 10 월

서울대학교 대학원

의학과 영상의학전공

최 영 훈

최영훈의 박사 학위논문을 인준함

2020 년 1 월

위 원 장 _____ (인)

부 위 원 장 _____ (인)

위 원 _____ (인)

위 원 _____ (인)

위 원 _____ (인)

Abstract

Evaluation of cerebral blood flow changes associated with cerebral hypoxia-ischemia in neonatal rats using arterial spin labeling perfusion MRI

Choi Young Hun

Radiology

The Graduate School

Seoul National University

Purpose

The purpose of this study was to evaluate cerebral blood flow (CBF) changes over time in the animal model of neonatal hypoxic-ischemic brain injury using arterial spin labeling (ASL) and correlate CBF changes with development of diffusion restriction on diffusion-weighted imaging (DWI).

Materials and methods

Six 7-day-old neonatal rats with unilateral carotid artery ligation underwent multiple ASL and DWI MRI scans at 9.4 T before and during hypoxia (8% O_2). One 7-day-old rat underwent ASL MRI without surgical ligation or hypoxia as a normal CBF control. Delayed T2-weighted MR imaging and histological examination were performed on day 3 post-hypoxia. CBF values on ASL were measured in four brain areas (i.e., ipsilateral and contralateral cortical and deep areas). The development of diffusion restriction was also evaluated in each of the four areas (i.e., DWI-positive[+] vs. DWI-negative[-] areas). Regional CBF changes over

time were evaluated. Regional CBF values and their changes over time were compared between the DWI(+) and DWI(-) areas.

Results

Regional CBF values before hypoxia were significantly lower than those of the normal control (CBF in normal control vs. CBF before hypoxia: 147.8 vs. 39.2 ± 19.7 in ipsilateral cortex, $p < 0.01$; 151.5 vs. 49.2 ± 21.2 in ipsilateral deep area, $p < 0.01$; 150.0 vs. 108.2 ± 22.2 in contralateral cortex, $p = 0.014$; and 165.0 vs. 104.22 ± 26.0 in contralateral deep area, $p < 0.01$). After exposure to hypoxia, CBF values decreased in all areas (mean CBF difference: -25.5 in ipsilateral cortex, $p = 0.057$; -21.5 in ipsilateral deep area, $p = 0.012$; -52.2 in contralateral cortex, $p<0.01$; -36.4 in contralateral deep area, $p<0.01$). Eleven areas with diffusion restriction were included in the DWI(+) area group, whereas 13 areas showing no diffusion restriction were included in the DWI(-) area group. The regional CBF values in the DWI(+) area were estimated to be 34.6 ml/100 g/min lower than those in the DWI(-) area. On delayed T2-weighted MRI, the diffusion-restricted areas presented as areas of bright signal intensity or heterogeneous mixed signal intensity with volume loss, which correlated to areas of infarction or ischemia on histology.

Conclusion

The ASL perfusion MRI technique made it possible to evaluate regional CBF changes over time during exposure to hypoxia in neonatal rats with unilateral carotid artery ligation. Damaged brain areas that matched well with the diffusion restricted areas had significantly lower CBF values at all time points, compared to preserved areas without diffusion restriction. CBFs measured with ASL may be utilized as a useful imaging indicator of subsequent hypoxic ischemic brain damage.

……

Keywords : Rice-Vannucci, perinatal hypoxia, hypoxic ischemic encephalopathy, cerebral blood flow, arterial spin labeling, perfusion magnetic resonance imaging

Student Number : 2011-31133

목차

Introduction

Brain damage resulting from perinatal cerebral hypoxia-ischemia is a major cause of acute mortality and chronic disability in infants and children. Between 20 to 50% of newborn infants with hypoxic-ischemic encephalopathy expire during the newborn period, and of the survivors, up to 25% exhibit permanent neuropsychological handicaps in the form of cerebral palsy with or without associated mental retardation, learning disability, or epilepsy (1). Given the magnitude of neonatal hypoxic-ischemic brain injury, it is appropriate that researchers have established relevant animal models and evaluated the pathophysiology underlying neonatal hypoxic-ischemic brain damage in those models.

The Rice-Vannucci model, an animal model of neonatal hypoxic-ischemic brain injury, was established in 1981 (2). The original Rice-Vannucci model was produced by ligating one carotid artery in a 7-day-old rat followed by exposing the animal to 8% oxygen at 37 °C for 3.5 h to induce ischemic neuronal changes. However, the procedure for the original model does not always lead to hypoxic-ischemic brain injury in neonatal rats and has a reported success rate between 56–79%, which indicates that there is significant inter- and intra-subject variability in the extent of the brain injury in the hypoxic-ischemic injury model: a subset of pups suffers no perceivable brain injury, while other pups suffer massive infarct (3, 4). The variability in animal models, however, makes results of preclinical studies difficult to analysis. Therefore, efforts have been made to offset this hindrance and, in particular, to exclude subjects with no lesion, but there is no widely used method to optimize the degree of brain injury. A few parameters such as apparent diffusion coefficient (ADC) obtained by magnetic resonance imaging (MRI) (5, 6) or blood flow assessed by color-coded pulsed Doppler ultrasound

imaging (3) have been used to exclude pups without a lesion at an early stage of brain injury.

Cerebral blood flow (CBF), which is measured as the volume of arterial blood (mL) delivered to 100 g of brain tissue per minute, reflects the process of nutritive delivery of arterial blood to the capillary beds within brain tissue. Accurate measurement and monitoring of CBF can provide important hemodynamic information on perinatal hypoxic-ischemic brain injuries. As a MRI technique for in vivo CBF quantification, arterial spin labeling (ASL) MRI indirectly measures CBF by magnetically tagging mobile protons within the cerebral arterial blood before they enter the tissue of interest (7). In a typical ASL experiment, the arterial blood is tagged by inverting the magnetization, and, after a delay, the tagged blood arrives at the image plane and an image is acquired. A control measurement is then made without tagging the arterial blood. If the tagged and control images are carefully adjusted so that the signal from the static spins is the same in both cases, then the difference in signal will be proportional to the amount of arterial blood delivered, and, thus, proportional to CBF. ASL has proven its feasibility in quantitative CBF measurements across species, from clinical functional MRI studies in humans to perfusion mapping in rat brains (8, 9).

The pathophysiology of perinatal hypoxic-ischemic brain injury is undoubtedly complex and remains incompletely understood. The majority of the underlying pathologic events are triggered by impaired cerebral blood flow and oxygen delivery to the brain (10). The principle pathogenetic mechanism resulting from hypoperfusion/hypoxia or both is deprivation of glucose and oxygen supply which initiates a cascade of biochemical events leading to cell dysfunction and ultimately to cell death (11). Therefore, evaluation of cerebral blood flow changes at the

initial stage of the injury would be very important to estimate the evolution of hypoxic-ischemic brain injury. However, until now, there have been a few studies regrading CBF changes in the perinatal hypoxic-ischemic brain injury animal model. Earlier studies regarding CBF changes in the Rice-Vannucci model used radioactive tracers and had to sacrifice rats in order to measure CBF (12, 13). Therefore, these studies could not evaluate CBF changes over time in one subject and did not reflect the diversity of inter-individual responses to hypoxia exposure. Consequently, studies crudely concluded that CBF decreased to 7 to 40% of control values at 1 to 3 hour of hypoxia. Several recent studies used optical imaging techniques such as laser Doppler flowmetry, laser speckle contrast imaging or diffuse correlation spectroscopy in order to measure cerebral hemodynamics in a noninvasive manner (14, 15). However, these techniques have a limited depth of penetration. Therefore, CBF monitoring of deep brain structures other than the superficial cortex is practically impossible in animals larger than rodents (16). In contrast, in vivo ASL MRI can repeatedly measure regional CBFs of the whole brain, including both superficial and deep brain areas at multiple time points (17, 18).

In this study, we tried to use the ASL perfusion MRI technique to evaluate regional CBF changes over time during exposure to hypoxia in neonatal rats with unilateral carotid artery ligation. Furthermore, in order to explain variable susceptibility to a hypoxic-ischemic insult in animal models, we correlated CBF changes with development of diffusion restriction on diffusion-weighted imaging (DWI) and later morphological brain injury evaluated on T2-weighted imaging and histology.

Materials and methods

The experiments were approved by the Seoul National University Animal Ethics Committee.

Animal preparation

Pregnant Sprague-Dawley rats were obtained approximately 1 week before parturition. Neonatal rats were kept under a regular light/dark cycle (lights on 8 am–8 pm) with free access to food and water for 7 d after birth. Seven-day-old rats, averaging between 12–14 g in weight, underwent unilateral ligation of the right common carotid artery (double ligation) via a midline neck incision after anesthesia with intraperitoneal injections of 80 mg/kg ketamine and 10 mg/kg xylazine. The surgery typically lasted for 5 min per rat, after which the rats were kept in an incubator for observation at 34 °C for approximately 15 min. After the rats stabilized, they were subsequently placed in a 9.4 T MRI bore and imaged. In the MRI bore, rats were anesthetized using 1.2% isoflurane with premixed gas consisting of 20% O_2 and 80% N_2. After obtaining the initial ASL and DWI scans, we lowered the oxygen content by changing the mixing ratio of the gas from 20% O_2 and 80% N_2 to 8% O_2 and 92% N_2 to create a hypoxic condition. For each rat, multiple ASL and DWI scans were obtained during hypoxia. We maintained the rats at a temperature of approximately 34 °C before, during, and after MR scanning. To avoid potential changes in cerebral blood perfusion during perfusion data collection, respiration was carefully monitored in the animals throughout the MR experiments.

MRI technique

ASL and DWI scans were performed before hypoxia and every 30 mins during hypoxia using a 9.4 T MR system (Agilent 9.4T/160AS; Agilent Technologies, Santa Clara, CA, USA) with a volume coil for radiofrequency (RF) transmission and phased-array 4-channel surface coil for signal reception (Agilent Technologies).

After the acquisition of routine, low-resolution scout images, automatic shimming was performed for the brain. Based on the scout images, one coronal slice intersecting the central region of the brain (bregma: 2.0 mm) was defined for the following DWI and ASL MRI scans.

For DWI, a fat-saturated DW four-shot spin-echo echo planar imaging (SE-EPI) sequence was used. The sequence parameters were as follows: b = 0/500/1000 s/mm^2, TR/TE = 3700/40 ms, field of view (FOV) = 22 × 22 mm, matrix size = 128 × 128, 5 slices, slice thickness = 1 mm, bandwidth = 250 kHz, and number of acquisitions = 2. The acquisition time for DWI was 1 min 30 s.

For ASL MRI, a flow-sensitive alternating inversion-recovery (FAIR) sequence (8, 19) was used with a single-shot SE-EPI readout. Selective and non-selective inversion were performed using a hyperbolic-secant adiabatic pulse (pulse duration = 6 ms and thickness = 3 mm). The post-labeling delay was 1400 ms. The other sequence parameters were as follows: TR/TE = 4000/29 ms, FOV = 18 × 17 mm^2, matrix size = 64 × 64, 1 slice, slice thickness = 1 mm, bandwidth = 250 kHz, and 60 repetitions of a pair of control and labeled scans. For quantitative analysis of cerebral blood perfusion, T1 and M_0 mapping was also performed using a fat-suppressed single-shot inversion-recovery (IR) SE-EPI sequence with TR/TE = 8000/29 ms and inversion times (TIs) = 25, 70, 150, 300, 600,

1000, 1800, and 2800 ms or 13, 31, 75, 181, 434, 1040, 2500, and 6000 ms. The acquisition time for ASL as well as T1 and M_0 mapping was approximately 10 min in total.

One 7-day-old rat underwent ASL MRI without surgical ligation or hypoxia and served as a normal CBF control.

Delayed MRI was performed on day 3 post-hypoxia using a 3.0 T MR system (TrioTim, Siemens). Coronal T2-weighted images were obtained with a fast SE sequence as follows: TR = 3000 ms, TE = 100 ms, FOV = 3.5 × 3.5 cm, slice thickness = 8 mm, slice spacing = 1.2 mm, acquisition matrix = 192 × 144, echo train length = 15, and number of acquisitions = 3. The acquisition time for T2-weighted imaging was approximately 3 min 8 s.

Histology

After the final MRI scan on day 3 post-hypoxia, all rats were euthanized. Rat brains were removed and cut into two parts at approximately 2 mm posterior to the bregma (i.e., the point where the frontal and parietal bones meet at the midline). The specimens were fixed in 10% neutral buffered formalin (pH 6.8–7.2) at room temperature. Coronal sections were cut along the same plane as the MRI slices and subsequently embedded in paraffin. One pathologist (H.M.J.) reviewed the 4-μm-thick sectioned hematoxylin-eosin stained slides and analyzed the histologyical findings.

Image analysis

From the ASL images, CBF maps were generated in ml/100 g/min

according to equation [1] in (20), assuming a tissue-blood partition coefficient of 0.9 ml/g (21), an inversion efficiency of 0.96, and arterial blood T1 of 2200 ms (22). A three-parameter fit was used to estimate T1 and M_0 maps. For DWI, apparent diffusion coefficient (ADC) maps were estimated by nonlinear least-squares fitting assuming a single exponential decay.

Using ASL CBF maps, one radiologist (Y.H.C. with 15 years of experience) measured regional CBF values in each of the four brain areas by drawing regions of interest (ROIs) as shown in Figure 1b. Two ROIs were placed on each side of the cerebral cortex. Two additional ROIs contained deep structures, including the thalamus, basal ganglia, and hippocampus. All image analyses were performed using Matlab (v. 9.5; Math Works, Inc., Natick, MA, USA).

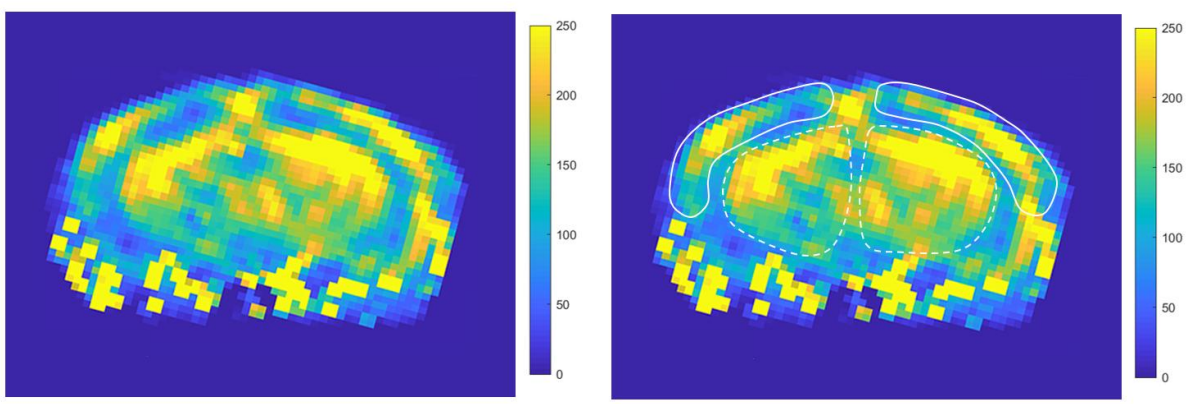

Figure 1. (a) Arterial spin labeling (ASL) cerebral blood flow (CBF) map obtained from a normal 7-day-old rat. (b) Representative image of regions of interest (ROIs) used for CBF quantification. ROIs with solid lines indicate the right and left cortices. ROIs with dotted lines indicate deep areas, including the thalamus, basal ganglia, and hippocampus.

At 1-week intervals, the radiologist (Y.H.C.) reviewed multiple DW images at multiple time points and determined the presence of diffusion restriction for each of the four brain areas. On ADC maps, diffusion restriction was considered to be present if an area showed a signal intensity < 80% of that of the normal area (23). The radiologist subjectively evaluated each of four areas on delayed T2-weighted images.

Statistical analysis

Brain areas showing positive diffusion restriction at any time point were grouped into the diffusion-positive (DWI(+)) area group, whereas brain areas with no diffusion restriction at all time points were grouped into the diffusion negative (DWI(-)) area group. CBF values before hypoxia at each brain area were compared with those of each brain area in the normal control rat using one-sample t-tests. CBF values before and immediately after (0 min post-hypoxia) hypoxia were compared using paired t-tests for each brain area. CBF values in diffusion-restricted areas were compared to those of areas without diffusion restriction using an independent t-test. CBF values were compared between DWI(+) and DWI(-) areas using a linear mixed model to account for repeated observations within subjects (i.e., subject-location-time) (24). A compound symmetry covariance matrix was used. The group (DWI(+) vs. DWI(-)), location (right cortex vs. right deep area vs. left cortex vs. left deep area), time, and group × time interaction were modeled as fixed effects, and the subject and location were treated as random effects. The model parameters were considered significant if the corresponding F-tests had P values < 0.05.

All data were analyzed with SPSS (SPSS for Windows, version 25.0; SPSS, Chicago, IL, USA) and SAS (version 9.2; SAS Institute Inc., Cary, NC, USA) statistical software packages. P values < 0.05 indicated statistical significance for all statistical tests.

Results

Seven 7-day-old rats successfully underwent surgery and MRI. Of these rats, one died (no abdominal respiration) during MRI and was excluded from the study. Therefore, six rats were included in the study. Of these rats, two rats (rats 1 and 4) showed diffusion restriction in the right cerebral cortex before hypoxia exposure. During hypoxia, three rats (rats 1, 2, and 3) developed new diffusion-restricted areas. In rat 1, the right cortical area showed diffusion restriction before hypoxia and continued to show diffusion restriction until the end of MRI at 180 min. Moreover, the right deep area showed diffusion restriction from 30 min post-hypoxia, whereas the left cortex showed diffusion restriction from 90 min post-hypoxia. The left deep area of rat 1 showed no diffusion restriction until the end of MRI at 180 min post-hypoxia. Rat 2 showed diffusion restriction in the right cortical and deep areas from 0 min post-hypoxia and the left cortical area from 60 min post-hypoxia until the end of MRI. Rat 3 showed diffusion restriction in the right cortical, right deep, and left cortical areas from 0 min post-hypoxia, and the left deep area showed diffusion restriction from 120 min post-hypoxia. The other three rats (rats 4, 5, and 6) showed no additional diffusion-restricted areas. Therefore, 11 areas with diffusion restriction were included in the DWI(+) area, whereas 13 areas without diffusion restriction were included in the DWI(-) area.

Rat 2 died immediately after MRI. Consequently, five rats underwent delayed MRI on day 3 post-hypoxia. The MRI timetable for each rat is presented in Table 1.

Rat	MRI acquisition time points	Diffusion-positive area: before hypoxia	Diffusion-positive area: during hypoxia
1	Pre-hypoxia, 0, 30, 60, 90, 120, 150, 180-min post-hypoxia Day 3 post-hypoxia	Right cortex	Right & left cortex Right deep areas
2	Pre-hypoxia, 0, 30, 60, 90-min post-hypoxia	None	Right & left cortex Right deep areas
3	0, 30, 60, 90, 120-min post-hypoxia Day 3 post-hypoxia	Not applied	Right & left cortex Right & left deep areas
4	Pre-hypoxia, 0, 30, 60, 90-min post-hypoxia Day 3 post-hypoxia	Right cortex	Right cortex
5	Pre-hypoxia, 0, 30, 60, 90-min post-hypoxia Day 3 post-hypoxia	None	None
6	Pre-hypoxia, 0, 30, 60-min post-hypoxia Day 3 post-hypoxia	None	None

Table 1. Magnetic resonance imaging (MRI) acquisition time points and diffusion-restricted areas before and during hypoxia for each of the six rats.

The CBF values obtained from the normal 7-day-old rat were 147.8 and 150.0 ml/100g/min for the right and left cerebral cortices, respectively, and 151.5 and 165.0 ml/100g/min for the right and left deep areas, respectively.

The graphs in Figure 2 present the CBF values obtained from six rats for each of the four areas before and during hypoxia.

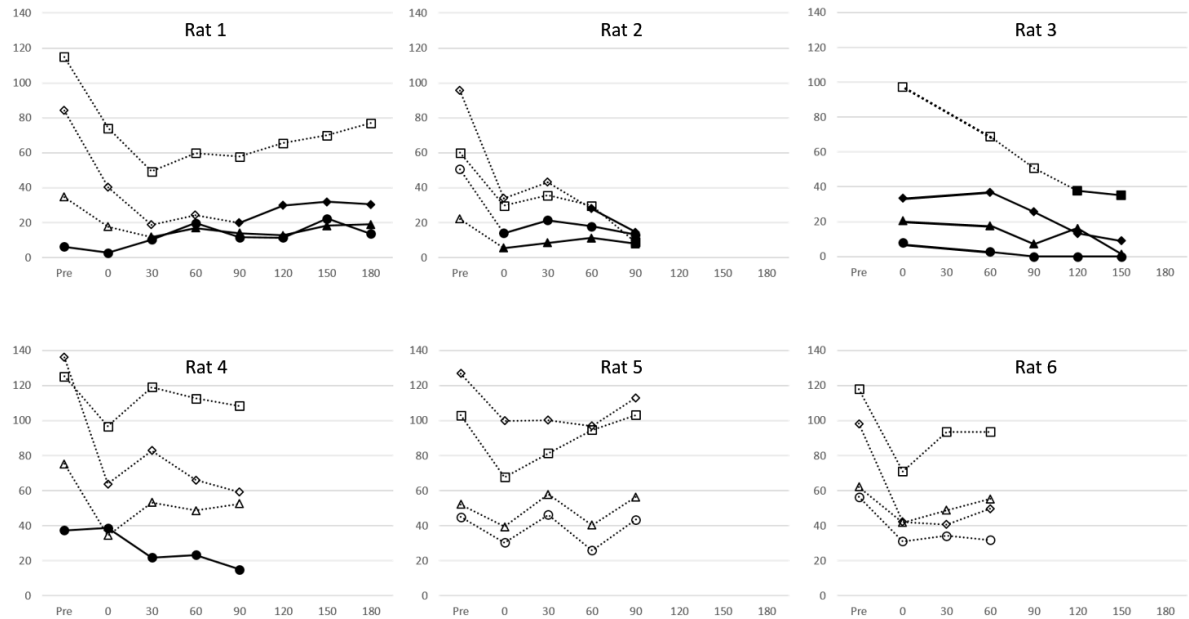

Figure 2. Cerebral blood flow (CBF) values over time for each of the four brain areas in six neonatal rats (○: right cortex, △: right deep area, ◇: left cortex, □: left deep area). Solid lines and symbols indicate the presence of diffusion restriction on diffusion-weighted images. *Y* axis, CBF in ml/100g/min and *X* axis, MRI acquisition time points.

CBF values were significantly lower than those of the normal control in all 22 brain areas (CBF in normal control vs. CBF before hypoxia: 147.8 vs. 39.2 ± 19.7 in the right cortex, $p < 0.01$; 151.5 vs. 49.2 ± 21.2 in the right deep area, $p < 0.01$; 150.0 vs. 108.2 ± 22.2 in the left cortex, $p = 0.014$; and 165.0 vs. 104.22 ± 26.0 in the left deep area, $p < 0.01$). CBF values decreased after exposure to hypoxia in all areas (mean CBF difference: -25.5 in the right cortex, $p = 0.057$; -21.5 in the right deep area, $p = 0.012$; -52.2 in the left cortex, $p < 0.01$; -36.4 in the left deep area, $p < 0.01$).

Areas with diffusion restriction (16.8 ± 10.7) showed significantly lower CBF values than areas without diffusion restriction (65.2 ± 30.9, $p < 0.01$). The maximum CBF in a diffusion-restricted area was 37.7 ml/100g/min.

After adjusting for subjects and locations (i.e., random effects), there were significant differences in CBF values according to group ($p < 0.001$), time ($p < 0.001$), and location ($p < 0.001$). The group × time interaction did not show statistical significance ($p = 0.455$). Specifically, the trend of CBF over time was not significantly different between the two groups. The regional CBF values in the DWI(+) area group were 34.6 ml/100g/min lower than those in the DWI(-) area group.

Covariate	Regression Coefficient	Standard Error of Estimate	p-value
Intercept	111.88	6.35	<.001
DWI (ref=negative)			
Positive	-34.66	5.77	<.001
TIME (ref=pre-hypoxia)			
0min post-hypoxia	-28.75	3.79	<.001
30min post-hypoxia	-26.24	3.92	<.001
60min post-hypoxia	-27.10	3.79	<.001
90min post-hypoxia	-30.53	4.01	<.001
120min post-hypoxia	-34.24	5.60	<.001
150min post-hypoxia	-34.04	5.60	<.001
180min post-hypoxia	-25.24	7.15	<.001
Location (ref=left deep area)			
Right cortex	-40.92	8.07	<.001
Right deep area	-37.70	7.89	<.001
Left cortex	-12.27	7.89	0.137

Table 2. Regression coefficients of fixed effects and intercept with standard errors (SEs) using a linear mixed effect model.

Table 3 and Figure 3 present the mean CBF values and their 95% confidence intervals for all time points in the DWI(+) and DWI(-) groups.

	Estimated CBF (mean±SE)		p-value†
	DWI(+) area	DWI(-) area	
Pre-hypoxia	54.49 ± 4.84	89.16 ± 4.68	<.001
0min post-hypoxia	25.74 ± 4.6	60.41 ± 4.6	
30min post-hypoxia	28.25 ± 4.84	62.91 ± 4.68	
60min post-hypoxia	27.39 ± 4.6	62.05 ± 4.6	
90min post-hypoxia	23.96 ± 4.69	58.62 ± 4.84	
120min post-hypoxia	20.25 ± 5.84	54.91 ± 6.28	
150min post-hypoxia	20.45 ± 5.84	55.11 ± 6.28	
180min post-hypoxia	29.25 ± 7.5	63.92 ± 7.71	

Table 3. Estimated mean cerebral blood flow (CBF) values with standard errors(SEs) over time for DWI-positive and DWI-negative area groups. †p-value using a linear mixed effect model

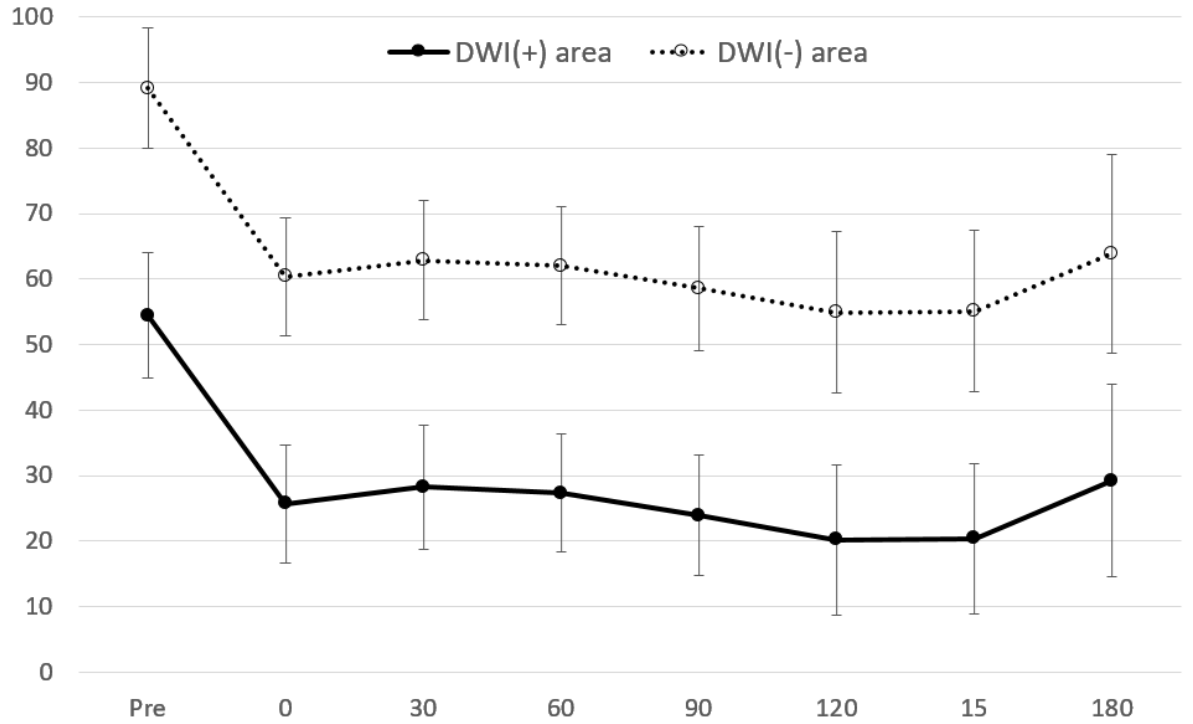

Figure 3. Mean cerebral blood flow (CBF) values with 95% confidence intervals over time for the DWI-positive and DWI-negative area groups. There are significant differences in the CBF values between the two groups at all time points ($p < 0.001$).

Two representative cases (rats 1 and 5) from the DWI(+) and DWI(-) area groups are presented in Figures 4 and 5.

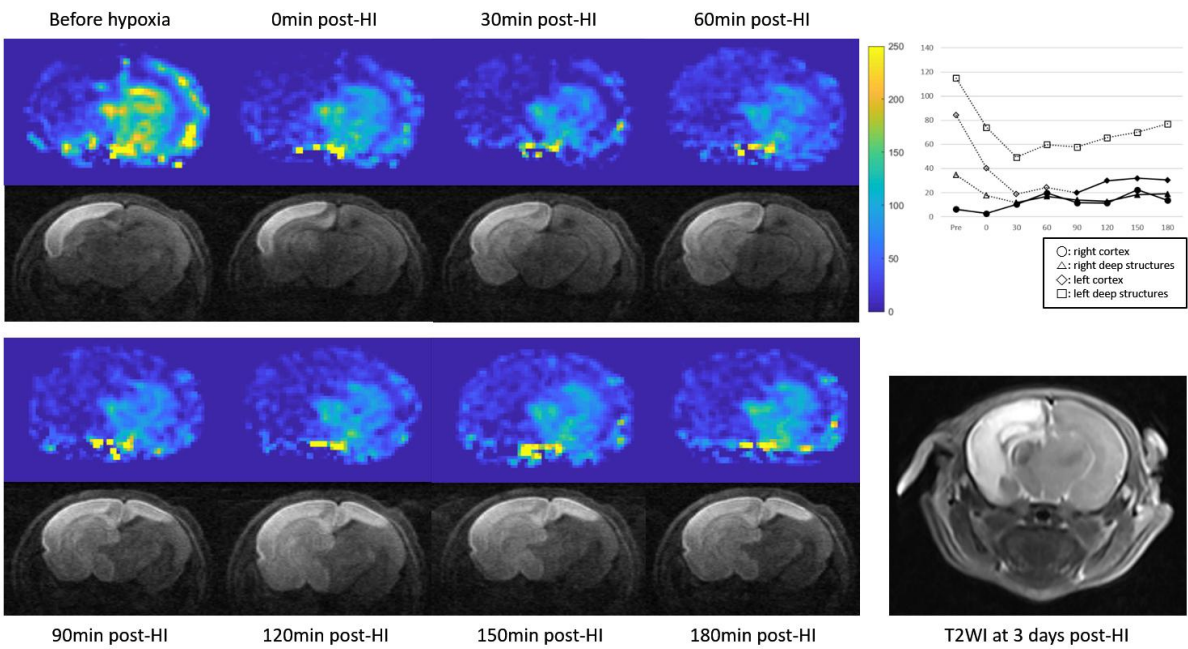

Figure 4. Representative case from the DWI-positive group (rat 1). The right cortex shows diffusion restriction before hypoxia. CBF generally decreases after exposure to hypoxia with areas of diffusion restriction extending through the right deep area and left cortex. The left deep area (a DWI-negative area) shows slow CBF recovery over time. The T2-weighted image (T2WI) on day 3 post-hypoxia reveals areas of bright high signal intensity and heterogeneous signal change with volume loss in the corresponding diffusion-restricted areas.

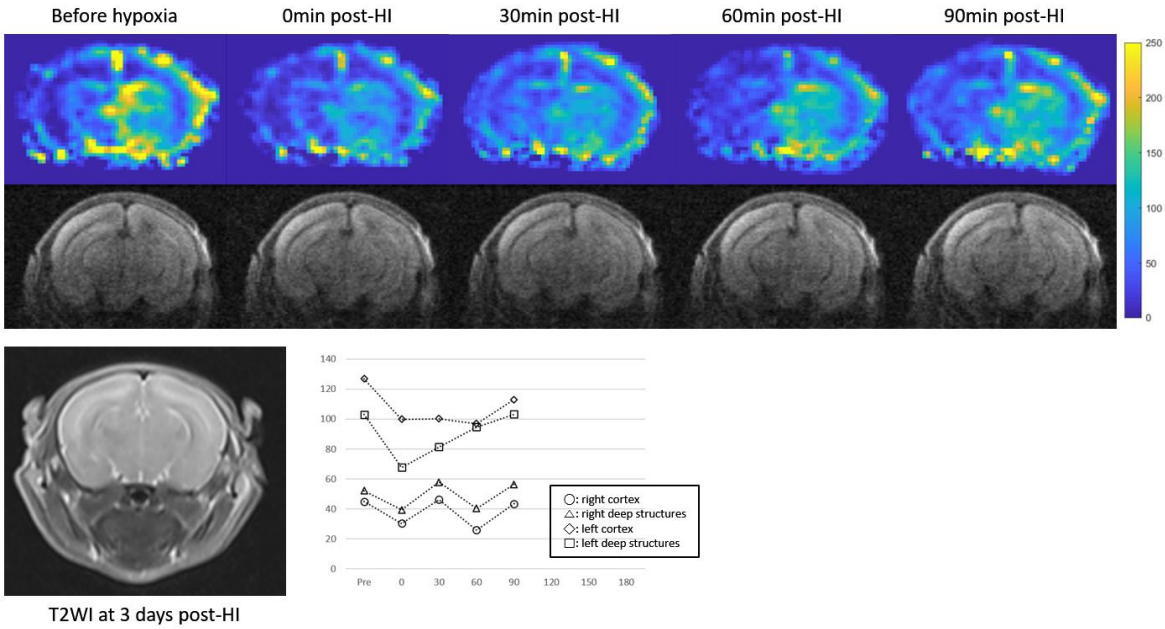

Figure 5. Representative case from the DWI-negative group (rat 5). CBF values before hypoxia were reduced compared to those of the normal control (see Fig. 1a). After exposure to hypoxia, CBF values in all brain areas were further diminished. However, the degree of CBF reduction does not appear to be as great as that shown in Figure 4. CBF values slowly and progressively increased over time. There were no areas of diffusion restriction or abnormalities detected on the follow-up T2-weighted image (T2WI) acquired on day 3.

On T2-weighted images obtained on day 3 post-hypoxia, diffusion-restricted areas appear as areas of cerebromalacia characterized by high signal intensity similar to water or areas of heterogeneous mixed signal intensity with volume loss. No abnormalities were observed in areas without diffusion restriction.

Hematoxylin and eosin–stained sections from the DWI(+) group revealed various degrees of ischemic change in diffusion-restricted areas. Frank infarction was noted in the areas corresponding to very high signal intensity areas on T2-weighted images acquired on day 3. The border zone areas between the infarction and normal tissue showed neuronal vacuolar changes and some pyknotic cells, which corresponded to areas with heterogeneous mixed signal intensity with mild volume loss (Fig. 6). In contrast, histological sections of the DWI(-) areas showed no gross abnormalities.

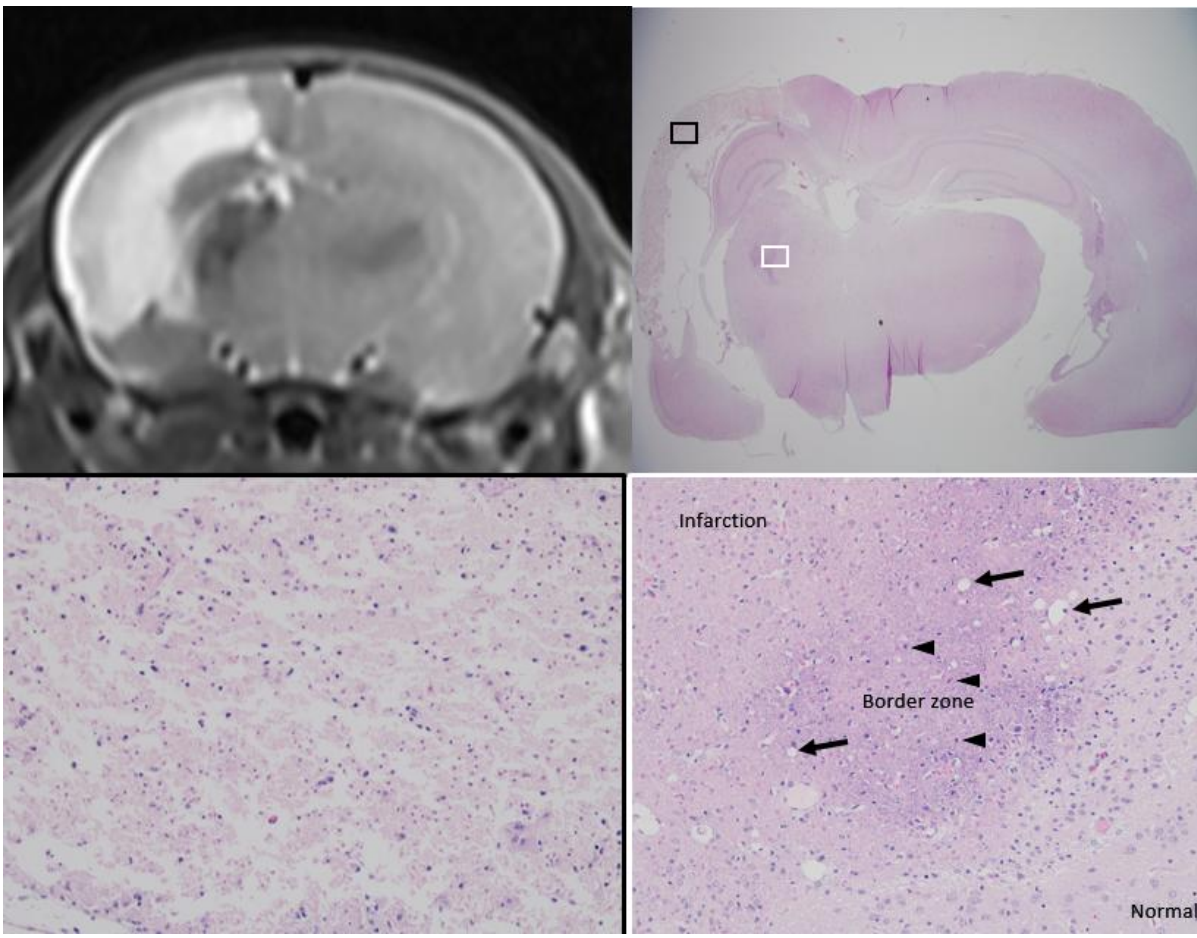

Figure 6. Radiological and histological correlation. (a) A coronal T2-weighted image at day 3 post-hypoxia shows areas of bright high signal intensity in the right cerebral cortex and part of the right deep area as well as heterogeneous signal change with volume loss in the right deep area. (b) Hematoxylin and eosin-stained brain section of the same rat (x1.25 magnification) reveals various degrees of ischemic change in areas of diffusion restriction. (c) Magnified view of the ipsilateral cortex (x20, black rectangular area in b) shows the frank infarction. (d) Magnified view of the border zone (x20, white rectangular area in b) shows neuronal vacuolar changes (arrows) and pyknotic cells (arrowheads).

Discussion

Over the past 20 years, the Rice-Vannucci model has been successfully used as an animal model of hypoxic-ischemic brain damage in the immature brain (25). At postnatal day 7, the rat brain is histologically similar to that of a 32- to 34-week gestation fetus or preterm infant. At this stage, cerebral cortical neuronal layering is complete, the germinal matrix is involuting, and white matter myelination is minimal. In this model, injury to both gray and white matters is usually induced (25). However, rats do not experience the same degree of hypoxic-ischemic brain damage with the Rice-Vannucci model. Although microscopic ischemic neuronal changes have been shown to occur in at least 90% of animals, infarction only occurred in 56% of brains according to a study by Rice et al (2). In another study using DWI to confirm brain injury induced by hypoxia-ischemia, 79% (23/27) of rats had evidence of brain injury at 1–2 h post-hypoxia-ischemia (23). Therefore, it is clear that there is individual variation in vulnerability to hypoxia-ischemia. Until now, CBF changes during hypoxia and individual variation in CBF changes in response to hypoxia-ischemia have not been evaluated in the rat model.

In this study, we used a FAIR sequence in neonatal rats for CBF quantification. The FAIR technique is a popular version of the pulsed ASL technique for rodent CBF measurements (22). FAIR is robust against magnetization transfer and eddy current effects (26). Using this ASL technique, we were able to evaluate CBF changes during hypoxia in neonatal rats and correlate these changes with those on DW images.

After unilateral carotid artery ligation without exposure to hypoxia, CBF values in the ipsilateral cortex and deep gray matter were 73 and 68% less than those of the normal control, respectively. Moreover, the CBF

values of the side contralateral to the ligation site were also decreased, with CBF decreasing by 28 and 37% in the contralateral cortex and deep gray matter, respectively. Similar trend of CBF reduction, i.e. CBF reduction in both hemispheres, but more marked in the ipsilateral hemisphere, has been noted in other prior studies (14, 15, 18). This may reflect the flow steal phenomenon caused by collateral blood supply to the ipsilateral side. After unilateral carotid artery ligation without exposure to hypoxia, diffusion restriction did not appear in 4/6 neonatal rats. Before exposure to hypoxia, two rats showed diffusion restriction in the ipsilateral cortex, which, of the four brain areas, was the region with the greatest decrease in CBF.

With exposure to hypoxia (8% O_2) after unilateral carotid artery ligation, a further decrease in the CBF values of all four brain areas occurred. This must have led to hypoperfusion in addition to hypoxia. With simultaneous development of hypoxia and hypoperfusion, diffusion restriction progressively evolved in 3/6 rats.

Contrary to many previous studies, in which chronic or subacute hypoxia led to an increase in CBF to maintain oxygen delivery to the brain (27), our study showed reduced CBF values with hypoxia exposure. A study by Qiao et al. showed a similar result of further CBF reduction in the ipsilateral hemisphere during hypoxia-ischemia (18). Even though these results are difficult to explain given the available data from this study, this may be CBF response to the acute hypoxia and is possibly related to a reduction in cardiac output due to cardiac ischemia and resultant systemic hypoperfusion. In one Rice-Vannucci model study, measurements of systemic physiological variables over the course of hypoxia showed a decrease in mean systemic blood pressure to a low of 23 mmHg (-23% from baseline) at 2 h (28). To confirm such a finding,

further studies would be necessary to monitor blood pressure in Rice-Vannucci models or review heart pathology.

Overall, the CBF responses to carotid artery ligation and hypoxia observed in our study seem to differ from those observed in previous studies (12, 13). In the first study to measure regional CBF using carbon-14 autoradiography with iodo-[^{14}C]-antipyrine as a radioactive tracer (13), hypoxia-ischemia was associated with decreases in regional CBF in the ipsilateral cerebral hemisphere such that, by 2 h, CBF values in the subcortical white matter, neocortex, striatum, and thalamus were 15, 17, 34, and 41% of control values, respectively. However, this study revealed that there was no significant decrease in CBF to the ipsilateral cerebral hemisphere by unilateral arterial occlusion alone. Another study evaluated regional CBF values using isopropyl-[^{14}C]-iodoamphetamine and showed that CBF to all regions of the ipsilateral cerebral hemisphere was not different from that of controls (no carotid artery ligation or hypoxia) at 10 and 20 min (12). Moreover, CBF values were decreased in all cerebral hemisphere structures ipsilateral to the carotid artery occlusion, ranging from 7 to 40% of control values after 1 h of hypoxia-ischemia. In contrast, our study found that CBF decreased with unilateral arterial occlusion alone and further decreased immediately after exposure to hypoxia. These findings may be due to technical limitations in measuring CBF using in vivo ASL MRI. In humans, CBF values have been underestimated in regions with delayed arterial transit times, especially in cerebrovascular occlusive diseases, such as Moyamoya disease (29). However, in rat experiments, the short transit times of rat cerebral vasculature and long T1 of blood at high field strength (9.4 Tesla) reduce the importance of transit time measurement (30). Furthermore, we used a post-labeling delay of 1400 ms, which is longer

than the reported arterial transit times of between 367–740 ms in rats with bilateral carotid artery occlusion (31). Therefore, the effect of arterial transit time delay on CBF measurement in neonatal rats with unilateral carotid artery occlusion might not be significant. Thus, we believe our results may reflect CBF changes more accurately than those of prior studies using radioisotopes. Prior studies needed to sacrifice rats to measure CBF values, which meant that each CBF data point was obtained from different subjects. Therefore, this data was likely to be affected by between-subject variation in CBF values. To confirm the CBF changes observed in our study, further studies that use a larger number of animals as well as more robust ASL techniques, such as multidelay ASL, will be required.

An important finding of our study was that diffusion restriction only developed in brain areas with persistently reduced CBF values that were below 37.7 ml/100 g/min. Our results agree with those of Shen et al. (32). In that study, the CBF viability threshold that best approximated pathological infarct volumes was 30 ± 9 mL/100 g/min (57 ± 11% reduction from baseline) in the permanent middle cerebral artery stroke rat model. These authors developed algorithms to predict ischemic tissue fate on a pixel-by-pixel basis using acute-phase CBF and ADC data. Based on the results of our study, a similar approach may be used. We think that we could use ASL CBF for predicting permanently damaged brain tissue in neonatal hypoxic-ischemic rat models. In that way, we could discriminate pups with and without a brain damage and diminish the variability in animal models.

An interesting finding of our study was that diffusion restriction did not occur in all rats, even though they were exposed to the same degree of hypoxia after unilateral carotid artery ligation. For rats with ischemia-

infarction, CBF values persistently decreased to < 37.7 ml/100 g/min. Non-affected rats also showed a decrease in CBF after hypoxia; however, their CBF values remained > 37.7 ml/100 g/min or temporarily (i.e., only at one time point) decreased below 37.7 ml/100 g/min. This finding may reflect individual variances in CBF responses to hypoxia. The mechanisms underlying the disturbance of CBF values in response to hypoxia are undoubtedly complex and likely multifactorial. In part, differences in hypoxia vulnerability may be related to individual variation in body temperature and sex effects (33). An examination of the factors leading to individual differences in CBF responses is beyond the scope of this study. However, future studies of factors affecting the degree of hypoxia-induced CBF reduction may reveal protective or aggravating effects on hypoxia vulnerability.

Another noteworthy finding of this study is that diffusion restriction progressed in a specific order and the CBF reduction hierarchy closely correlated with the distribution and progression of hypoxic-ischemic brain damage. When exposed to prolonged hypoxia, diffuse restriction progressed from the ipsilateral cortex to the ipsilateral deep area and then from the contralateral cortex to the contralateral deep area, similar to the order of decreased regional CBF values. Similarly, in human neonates, brain areas with lower baseline CBF values (i.e., the periventricular white matter in preterm infants and parasagittal intervascular boundary zones in term infants) are more vulnerable to mild to moderate hypoperfusion. Therefore, we believe that the ASL technique could be used to optimize and modulate the extent of brain injury and enable the analysis of the effect of an intervention on temporal and spatial changes in CBF so that mechanisms of neuroprotection can be assessed.

Finally, in our study, areas of diffusion restriction on DW images and areas of cystic change and heterogeneous signal alteration on T2-weighted images correlated well with histological areas of ischemia-infarction. Several prior studies have shown similar results. Wang et al. (23) compared infarction volumes measured on ADC maps at 1–2 h post-hypoxia-ischemia to those determined from histopathology. This study demonstrated that the size of the irreversible infarction on DWI at 1–2 h post-hypoxia-ischemia correlated moderately well with that on histopathology (r = 0.738). T2-weighted images obtained 24 h or more after a hypoxia-ischemia episode have been shown to represent tissue damage well when compared with histopathology (23, 34). On day 4 post-hypoxia-ischemia, lesion volumes on T2-weighted images significantly correlated with irreversible infarct volumes on histology (23).

Conclusion

In conclusion, with the ASL perfusion MRI technique, we were able to evaluate regional CBF changes over time during exposure to hypoxia in neonatal rats with unilateral carotid artery ligation. CBF values decreased on the contralateral side as well as on the ipsilateral side after unilateral carotid artery ligation without exposure to hypoxia and further decreased in all brain areas following hypoxia exposure. Damaged brain areas that matched well with the diffusion restricted areas had significantly lower CBF values at all time points, compared to preserved areas without diffusion restriction. CBFs measured with ASL may be utilized as a useful imaging indicator of subsequent hypoxic ischemic brain damage.

참고문헌

1. Vannucci RC, Vannucci SJ. Perinatal hypoxic-ischemic brain damage: evolution of an animal model. Dev Neurosci. 2005;27(2-4):81-6.
2. Rice JE, 3rd, Vannucci RC, Brierley JB. The influence of immaturity on hypoxic-ischemic brain damage in the rat. Ann Neurol. 1981;9(2):131-41.
3. Bonnin P, Leger PL, Deroide N, Fau S, Baud O, Pocard M, et al. Impact of intracranial blood-flow redistribution on stroke size during ischemia-reperfusion in 7-day-old rats. J Neurosci Methods. 2011;198(1):103-9.
4. Sheldon RA, Sedik C, Ferriero DM. Strain-related brain injury in neonatal mice subjected to hypoxia-ischemia. Brain Res. 1998;810(1-2):114-22.
5. Derugin N, Wendland M, Muramatsu K, Roberts TP, Gregory G, Ferriero DM, et al. Evolution of brain injury after transient middle cerebral artery occlusion in neonatal rats. Stroke. 2000;31(7):1752-61.
6. Wendland MF, Faustino J, West T, Manabat C, Holtzman DM, Vexler ZS. Early diffusion-weighted MRI as a predictor of caspase-3 activation after hypoxic-ischemic insult in neonatal rodents. Stroke. 2008;39(6):1862-8.
7. Buxton RB. Quantifying CBF with arterial spin labeling. J Magn Reson Imaging. 2005;22(6):723-6.
8. Kim SG. Quantification of relative cerebral blood flow change by flow-sensitive alternating inversion recovery (FAIR) technique: application to functional mapping. Magn Reson Med. 1995;34(3):293-301.
9. Detre JA, Zhang W, Roberts DA, Silva AC, Williams DS, Grandis DJ, et al. Tissue specific perfusion imaging using arterial spin labeling. NMR Biomed. 1994;7(1-2):75-82.
10. Allen KA, Brandon DH. Hypoxic Ischemic Encephalopathy: Pathophysiology and Experimental Treatments. Newborn Infant Nurs Rev. 2011;11(3):125-33.
11. Lai M-C, Yang S-N. Perinatal Hypoxic-Ischemic Encephalopathy. Journal of Biomedicine and Biotechnology. 2011;2011.
12. Ringel M, Bryan RM, Vannucci RC. Regional cerebral blood flow during hypoxia-ischemia in the immature rat: comparison of iodoantipyrine and iodoamphetamine as radioactive tracers. Brain Res Dev Brain Res. 1991;59(2):231-5.
13. Vannucci RC, Lyons DT, Vasta F. Regional cerebral blood flow during

hypoxia-ischemia in immature rats. Stroke. 1988;19(2):245-50.
14. Buckley EM, Patel SD, Miller BF, Franceschini MA, Vannucci SJ. In vivo Monitoring of Cerebral Hemodynamics in the Immature Rat: Effects of Hypoxia-Ischemia and Hypothermia. Dev Neurosci. 2015;37(4-5):407-16.
15. Ohshima M, Tsuji M, Taguchi A, Kasahara Y, Ikeda T. Cerebral blood flow during reperfusion predicts later brain damage in a mouse and a rat model of neonatal hypoxic-ischemic encephalopathy. Exp Neurol. 2012;233(1):481-9.
16. Devor A, Sakadzic S, Srinivasan VJ, Yaseen MA, Nizar K, Saisan PA, et al. Frontiers in optical imaging of cerebral blood flow and metabolism. J Cereb Blood Flow Metab. 2012;32(7):1259-76.
17. Meng S, Qiao M, Scobie K, Tomanek B, Tuor UI. Evolution of magnetic resonance imaging changes associated with cerebral hypoxia-ischemia and a relatively selective white matter injury in neonatal rats. Pediatr Res. 2006;59(4 Pt 1):554-9.
18. Qiao M, Latta P, Foniok T, Buist R, Meng S, Tomanek B, et al. Cerebral blood flow response to a hypoxic-ischemic insult differs in neonatal and juvenile rats. MAGMA. 2004;17(3-6):117-24.
19. Kwong KK, Chesler DA, Weisskoff RM, Donahue KM, Davis TL, Ostergaard L, et al. MR perfusion studies with T1-weighted echo planar imaging. Magn Reson Med. 1995;34(6):878-87.
20. Pell GS, Thomas DL, Lythgoe MF, Calamante F, Howseman AM, Gadian DG, et al. Implementation of quantitative FAIR perfusion imaging with a short repetition time in time-course studies. Magn Reson Med. 1999;41(4):829-40.
21. Silva AC, Kim SG, Garwood M. Imaging blood flow in brain tumors using arterial spin labeling. Magn Reson Med. 2000;44(2):169-73.
22. Zheng B, Lee PT, Golay X. High-sensitivity cerebral perfusion mapping in mice by kbGRASE-FAIR at 9.4 T. NMR Biomed. 2010;23(9):1061-70.
23. Wang Y, Cheung PT, Shen GX, Wu EX, Cao G, Bart I, et al. Hypoxic-ischemic brain injury in the neonatal rat model: relationship between lesion size at early MR imaging and irreversible infarction. AJNR Am J Neuroradiol. 2006;27(1):51-4.
24. Fitzmaurice GM, Laird NM, Ware JH. Applied longitudinal analysis. Hoboken, N.J.: Wiley-Interscience; 2004. xix, 506 p. p.
25. Choi EK, Park D, Kim TK, Lee SH, Bae DK, Yang G, et al. Animal models

of periventricular leukomalacia. Lab Anim Res. 2011;27(2):77-84.
26. Bernstein MA, King KF, Zhou ZJ. Handbook of MRI pulse sequences. Amsterdam ; Boston: Academic Press; 2004. xxii, 1017 p. p.
27. Harris AD, Murphy K, Diaz CM, Saxena N, Hall JE, Liu TT, et al. Cerebral blood flow response to acute hypoxic hypoxia. NMR Biomed. 2013;26(12):1844-52.
28. Welsh FA, Vannucci RC, Brierley JB. Columnar alterations of NADH fluorescence during hypoxia-ischemia in immature rat brain. J Cereb Blood Flow Metab. 1982;2(2):221-8.
29. Wang R, Yu S, Alger JR, Zuo Z, Chen J, Wang R, et al. Multi-delay arterial spin labeling perfusion MRI in moyamoya disease--comparison with CT perfusion imaging. Eur Radiol. 2014;24(5):1135-44.
30. Alsop DC, Detre JA. Reduced transit-time sensitivity in noninvasive magnetic resonance imaging of human cerebral blood flow. J Cereb Blood Flow Metab. 1996;16(6):1236-49.
31. Thomas DL, Lythgoe MF, van der Weerd L, Ordidge RJ, Gadian DG. Regional variation of cerebral blood flow and arterial transit time in the normal and hypoperfused rat brain measured using continuous arterial spin labeling MRI. J Cereb Blood Flow Metab. 2006;26(2):274-82.
32. Shen Q, Meng X, Fisher M, Sotak CH, Duong TQ. Pixel-by-pixel spatiotemporal progression of focal ischemia derived using quantitative perfusion and diffusion imaging. J Cereb Blood Flow Metab. 2003;23(12):1479-88.
33. Vannucci SJ, Hagberg H. Hypoxia-ischemia in the immature brain. J Exp Biol. 2004;207(Pt 18):3149-54.
34. Qiao M, Malisza KL, Del Bigio MR, Tuor UI. Transient hypoxia-ischemia in rats: changes in diffusion-sensitive MR imaging findings, extracellular space, and Na+-K+ -adenosine triphosphatase and cytochrome oxidase activity. Radiology. 2002;223(1):65-75.

요약(국문초록)

신생 백서를 이용한 저산소성 허혈성 뇌손상 모델에서 동맥스핀표지 관류 자기공명영상법을 통한 뇌혈류 변화 평가

목적

신생 백서를 이용한 저산소성 허혈성 뇌손상 모델에서 동맥스핀표지(ASL) 관류자기공명영상을 이용하여 시간 경과에 따른 대뇌혈류(CBF)의 변화를 평가하고, 뇌혈류 변화와 확산강조영상(DWI) 및 조직학적 소견을 비교 평가하고자 한다.

방법

생후 7일된 신생아 쥐 6마리에서 일측 경동맥을 결찰한 뒤 저산소(8% O2)를 가하면서 9.4T MRI에서 ASL 및 DWI MRI 검사를 시행하였다. 생후 7일된 쥐 한 마리를 외과적 결찰이나 저산소증없이 ASL MRI를 시행하여 정상 뇌혈류 대조군으로 사용하였다. 3일 뒤 T2강조영상과 조직검사를 시행하였다. ASL CBF 값을 4개의 뇌영역(즉, 동측과 반대측 피질 및 심부 영역)에서 측정하였다. 각 영역에서 DWI상 제한확산의 발생 여부를 평가하였다 (즉, DWI-양성 대 DWI-음성군). 시간 경과에 따른 CBF 변화를 평가하였다. 시간 경과에 따른 CBF 변화 양상을 DWI양성군과 음성군간에 비교하였다.

결과

일측 경동맥 결찰 후 CBF 값은 정상 대조군에 비해 유의하게 낮아졌다 (정상 대조군 CBF vs.대 저산소증 전 CBF: 동측 대뇌피질, 147.8 vs. 39.2 ± 19.7, p <0.01; 동측 심부영역, 151.5 vs. 49.2 ± 21.2, p <0.01; 반대측 피질, 150.0 vs. 108.2 ± 22.2, p = 0.014; 반대측 심부영역, 165.0 vs 104.22 ± 26.0, p <0.01). 저산소에 노출 된 후 CBF 값은 모든 영역에서 감소했다 (평균 CBF 차이, 동측 피질에서 -25.5, p = 0.057; 동측 심부영역에서 -21.5, p = 0.012, 반대쪽 피질에서 -52.2, p <0.01, 반대측 심부영역에서 -36.4, p <0.01). DWI양성군에는 확산제한이 있는 11개의 영역이 포함되었고 DWI음성군에는 확산제한이 없었던 13개의 영역이 포함되었다. DWI-양성군의 CBF 값은 DWI-음성군보다 평균 34.6 ml/100g/min 낮

았다. 지연 T2강조 MRI에서 확산 제한을 보였던 영역은 밝은 신호 강도 또는 부피 감소를 동반한 혼합 신호 강도 영역으로 보였으며 조직학상의 경색이나 허혈 영역과 일치하였다.

결론

ASL 관류자기공명영상법을 이용하여 신생백서에서 일측 경동맥 동맥 결찰 후 저산소증에 노출되는 동안, 시간에 따른 CBF 변화를 평가할 수 있었다. 확산 제한 영역과 잘 일치하는 손상 뇌영역은 확산 제한이 없었던 보존 뇌영역에 비해 모든 시점에서 CBF 값이 현저히 낮았다. ASL 기법으로 측정된 CBF값은 향후 저산소성 허혈성 뇌 손상 발생을 예측하는 데 유용한 영상지표로서 이용될 수 있다.

……..

주요어 : Rice-Vannucci, 주산기 저산소증, 저산소성 허혈성 뇌손상, 뇌혈류, 동맥스핀표지, 관류자기공명영상, 신생백서

학 번 : 2011-31133

감사의 글

부족한 저를 가르치시고 지도해주신 존경하는 김인원, 김우선, 천정은 교수님께 진심으로 감사드립니다. 인생의 귀감이 되는 훌륭한 선생님들 밑에서 배움의 기회를 얻을 수 있다는 것은 저에게는 정말 큰 행운으로 생각됩니다. 앞으로도 더욱 정진하여 선생님들께 누가 되지 않도록 노력하겠습니다.

또한 논문을 완성하는 데 큰 도움을 준, 사랑하는 아내이자 병리과 전문의 전혜민과 큰 기쁨인 딸 정원이에게 사랑하고 고맙다는 말을 전하고 싶습니다. 마지막으로 저를 이 세상에 있게 해 주신 부모님께도 깊이 감사드립니다.

2020년 1월

최영훈 올림